2012

A Hybrid Ray-Racing and Radiosity Method for Calculating Radiation Transport and Illuminance Distribution in Spaces With Venetian Blinds

Ying-Chieh Chan
ychan@purdue.edu

Athanasios Tzempelikos

A Hybrid Ray-Racing and Radiosity Method for Calculating Radiation Transport and Illuminance Distribution in Spaces with Venetian Blinds

Ying-Chieh Chan*, Athanasios Tzempelikos

School of Civil Engineering, Purdue University,
West Lafayette, IN, USA, Tel: 7865-496-7586, E-mail: ychan@purdue.edu

ABSTRACT

This paper presents a hybrid ray-tracing and radiosity method for processing luminous flux in spaces equipped with venetian blinds. The method considers both diffuse and specular characteristics of blinds and aims to establish a balance between computational speed and accuracy. Specular components are treated using ray-tracing techniques using a shining factor for the blinds to split between directly and diffusely reflected components. The direct components are traced inside the blind cavity and inside the room while the direct-diffuse components inside the blind cavity are processed in a two-dimensional radiosity calculation until the final diffuse flux departing the cavity is determined. Diffuse-to-diffuse transmission is considered using a traditional radiosity method. Each room surface is divided into sub-surfaces and given an initial luminous exitance, after accounting for directly traced portions. Then a 3-D radiosity method is employed for the entire room to compute illuminance distributions on each sub-surface and on the work plane. The developed model will help in the estimation of daylight distributions in spaces with venetian blinds and potential lighting energy savings calculations if combined with electric lighting controls. It will also lead to development of new control algorithms for shading and lighting systems for perimeter spaces with controllable shading devices.

1. INTRODUCTION

Daylighting is an important factor that impacts building energy consumption and occupants' visual comfort. To fully utilize daylighting, building perimeter zones are built and designed with window systems which include both glazing and shading devices. Venetian blinds are one of the most common shading systems widely used in commercial buildings. They consist of many horizontal rotatable slats and have well-built abilities to control the amount of illuminance transmitted into the room (and its direction) and the illuminance distribution on the work plane. The optical properties of venetian blinds are influenced by the solar incidence angle, slat tilt angle, and the surface optical characteristics of slats. Some materials have polished and smooth surfaces which are associated with high specular reflectance. The light rays striking on reflective slats will reflect following the laws of reflection. On the other hand, slat surfaces with high roughness will result in anisotropic reflection and mixed reflection patterns.

To optimize the usage of venetian blinds, we need to know the optical properties and the complete transmission characteristics also in order to predict the illuminance distribution on interior surfaces impacted by blinds. To solve the complex problem of blind transmittance, both EnergyPlus (LBNL, 2007) and ISO15099 (ISO, 2003) used a radiosity method which cut each slat to small pieces and assumed the slats were perfect diffusers. Some simplifications which reduce the surface numbers or simplify the model structure (Robinson and Stone, 2006, Kotey et al., 2009) or complications which considered the curvature and thickness of slats (Rosenfeld et al., 2001, Tzempelikos, 2008, Chaiyapinunt and Worasinchai, 2009) were made based on the radiosity model. However, it showed a bias when dealing with high specular surface (Versluis, 2005). For the slats with specular characteristics, 2-D analytical models (Parmelee and Aubele, 1952, Pfrommer, Lomas and Kupke, 1996) were developed. In Parmelee's model, the results were presented in either perfect diffuse models or perfect specular models with infinite inter-reflections between the slats. In Pfrommer's model, diffuse properties and specular properties were combined into a single model using a "shining factor" but only considered with two bounces inside the slats. Advanced experimental approaches (Simmler and Binder, 2008) such as bi-directional transfer function (Klems and Warner, 1995, Breitenbach et al., 2001, Andersen et al., 2005) were implemented to get accurate results for specific products and to validate the simulation results. To obtain the detailed interior illuminance distribution, the directional information of light should be kept in the calculation process. The 3-D ray tracing method which was originally developed in the computer graphics field was employed in complex fenestration system calculations. RADIANCE (Ward and Shakespeare, 1998) which is based on backward ray tracing algorithms is a powerful tool to compute accurate and detailed illuminance distributions. The concept of backward ray tracing presents what the observer sees

by emitting rays from the eye or the reference point back to the light source. The Monte-Carlo method, a sophisticated sampling method, was usually combined with ray tracing calculations in ray samples generating process (Tsangrassoulis et al., 2002). Therefore, forward ray-tracing algorithms were also used to provide more intuitive and full-scale results of illuminance distributions in the entire room (Campbell and Whittle, 1997, Andersen and de Boer, 2006). The disadvantage of pure ray tracing methods is that they are time-consuming and require heavy computational power and large computational memory, especially for surfaces with strong diffuse characteristics (large amount of rays should be sampled to accurately model anisotropic effects in the ray tracing process). Rapid algorithms such as radiosity-based methods were suggested for some cases (Lehar and Glicksman, 2007).

The objective of this paper is to present a hybrid ray-tracing and radiosity method for calculation of venetian blinds transmittance and interior illuminance distributions for rooms equipped with venetian blinds on the windows, in an efficient and accurate way. The method considers both diffuse and specular characteristics of the blinds and aims to establish a balance between computational speed and accuracy. The developed model will help in the estimation of daylight distributions in spaces with venetian blinds and potential lighting energy savings calculations if combined with electric lighting controls. It will also lead to development of new control algorithms for shading and lighting systems for perimeter spaces with controllable shading devices.

2. METHODOLOGY

Ray tracing and radiosity are both popular algorithms used to predict indoor daylighting distributions. Ray-tracing algorithms are appropriate when surfaces have ideal specular properties, whereas radiosity-based methods are suitable when dealing with diffuse properties (Lambertian surfaces are assumed). In the developed hybrid method, we use the ray-tracing method to capture the specular characteristics and the radiosity method to capture the diffuse characteristics of slat surfaces (and room interior surfaces if needed). The surfaces that have strong diffuse characteristics (such as a common interior wall) were only solved by the radiosity method. The surfaces that have both diffuse and specular characteristics were split to an anisotropic part (specular) which is solved by the ray tracing method and an isotropic part (diffuse) which solved by the radiosity method. The concept of a "shining factor" is used to split these two characteristic. The shining factor is defined as the ratio between the diffuse-reflected portion and the total-reflected portion (1 represents a perfect diffuser and 0 represents an ideal specular reflector). The concept was brought up by (Pfrommer et al., 1996) and originated from the measurement results by Ward which provided the diffuse reflectance and specular reflectance of some common materials (Ward, 1992).

Figure 1 presents a flowchart view of the hybrid ray-tracing and radiosity method that was developed for spaces equipped with venetian blinds on the windows. Daylight transmitted through glass consists of two parts – diffuse illuminance and direct illuminance. In this hybrid method, the diffuse part is treated with two-dimensional radiosity calculations and the direct part is treated with ray-tracing calculations –both for processing the luminous flux through the slats. The transmitted diffuse illuminance (we call it original diffuse component to distinguish it from other diffuse components) is assumed to be received uniformly from the sky and the ground and is processed with a 2-D radiosity matrix for transmission through the blinds. This calculation module with compute the amount of diffuse illuminance transmitted to inside and the amount reflected back to the glass, as well as the diffuse-to-diffuse transmittance of the blinds with the current slat tilt angle.

In the ray tracing method for direct illuminance calculation, there are three possible collision locations as illustrated in Figure 2: (i) light rays may first strike on the slat and are then inter-reflected between adjacent slats until they reach an interior surface or the glass (ii) light rays may first strike on a slat and are then reflected on the glass and (iii) light rays may be directly transmitted through the blinds and first strike on interior room surfaces. If the ray strikes on slat as shown in Figure 2(a), the impact of shining factor will be considered; the ray's representing illuminance attribution will be split between the direct-specular component and the direct-diffuse component. The amount of direct-diffuse component is accumulated in the inter-reflecting process inside the slats and then used into a 2-D radiosity module for prediction of the amount of light when the ray exits the slat cavity. The 2-D radiosity method is the same to the one used to treat the original diffuse component but with different initial exitance and surface segments. The direct-specular component is tracked continuously until it reaches the window or an interior wall. Figure 2(b) shows the case when the ray first strikes on the slat and is then reflected on the glass. When it strikes the glass, to simplify the calculation process, it loses the directional information and it is assumed to be perfectly diffuse. Consequently, we have three components reflected back on the glass: the reflected original diffuse component, the reflected direct-diffuse component (diffuse component generated in the inter-reflection process), and the direct-specular component. These three components are summed, part of them is transmitted back to outside, and part of them is reflected back towards the interior by the glass. The latter part is processed with inter-reflections between blinds and glass. The final diffuse component includes the transmitted amount from the 2-D radiosity method and the transmitted amount after several inter-reflections within the blind cavity. Figure 2(c) shows the case

when the ray is directly transmitted through the blinds and first strikes on an interior wall. Once arriving at an interior sub-surface (tracked with one-bounce ray-tracing), the percentage of this direct component that is reflected is used as the initial luminous exitance of that sub-surface in the 3-D radiosity method that is then performed for the room. If there is a directly-reflected component (from the specular blind reflection) on an interior sub-surface, it is also considered in its initial luminous exitance. The total diffuse transmitted light through the blinds is considered as the initial luminous exitance of the window-blind system in the 3-D room radiosity calculations to obtain the final illuminance distributions and work plane illuminances. In the above analysis, that slats are assumed to be flat and without significant thickness. Direct transmission through blinds of different curvatures and thickness was studied by Tzempelikos (2008). Finally, the interior room surfaces (except for the blinds) are assumed Lambertian (except if needed otherwise and a ray-tracing sub-module can be employed).

Figure 1: Process of the developed hybrid ray-tracing and radiosity method.

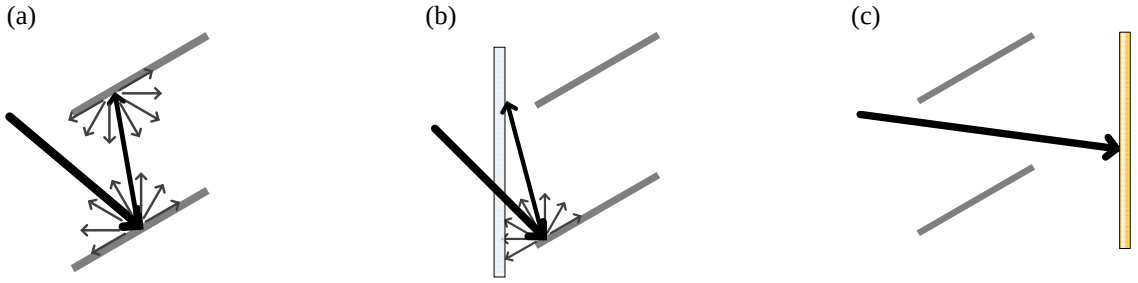

Figure 2: Possible scenarios for treating direct/specular transmission and reflection: (a) light rays first strike on the slat and are then inter-reflected between adjacent slats (ii) light rays first strike on a slat and are then reflected on the glass and (iii) light rays may be directly transmitted through the blinds and first strike on interior room surfaces.

2.1 Ray Tracing Module

For the direct components, a ray tracing method is employed to track the sun's projection area (if light is directly transmitted through blinds) and the shining factor is used to split between the direct and diffuse portions during every strike on the slats. All the points, planes (including all the slats and building interior surface), and rays were defined in a three-dimensional Cartesian coordinate system before starting to trace the rays. A certain number of

rays are randomly generated (Monte-Carlo sampling algorithm) from the light source (the window in this case) with a uniformly distributed generating probability. Each of the rays represents certain amount of direct luminous flux entering the room as described by Eq. (1).

$$\text{luminous flux in each ray} = \frac{\tau_{dir-win} E_{dir} A_{win}}{RayNum_{Total}} \tag{1}$$

where $\tau_{dir\text{-}win}$ is the direct window transmittance, E_{dir} is incident direct illuminance, A_{win} is the window area, and $RayNum_{Total}$ is the total generated number of rays. The latter has an effect on the accuracy of simulation results- a larger number provides more accurate results but also requires larger memory and calculation time. By analyzing the transmittance calculated by different ray numbers, we choose 5000 rays per square meter for this study. In the 3D Cartesian coordinate system, X-axis represents the north-south axis, Y-axis represents the east-west axis, and Z-axis represents the vertical (height) axis. Each of the rays is expressed as a position vector (which indicates the generated position) and a directional vector (which indicates the direction of the ray). The direction of the ray is based on the solar position and corresponding solar angle at the target time as shown in Figure 3 and expressed in Eq. (2):

$$\vec{T} = \left(\cos(\alpha)\cos(\phi),\quad \cos(\alpha)\sin(\phi),\quad -\sin(\alpha)\right) \tag{2}$$

where $\vec{T}$ is the directional vector of sun's rays, α is the solar altitude, and ϕ is the solar-surface azimuth. If the incident angle is greater than 90 degrees or less than 0 degrees, it means there is no direct illuminance on the window at that time and this step can be skipped to save computing time. Each of the interior walls is viewed as a plane and defined with a position vector (which can be any point lying on the plane) and a normal vector which indicates the direction of the plane. Following the reflection law of ideal specular surfaces, the incident angle is equal to the reflection angle. The travel distance from the ray's starting point to each plane (all the slats and interior surfaces) is computed using the following equations and is briefly described in Figure 4.

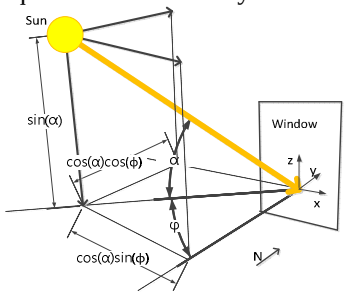

Figure 3: Corresponding solar angles and directional vector of light rays

$$\vec{R} = \vec{T} - 2(\vec{T}\cdot\vec{N})\vec{N} \tag{3}$$

$$t = \frac{(\vec{P}-\vec{Q})\cdot\vec{N}}{\vec{R}\cdot\vec{N}} \tag{4}$$

where $\vec{R}$ is the directional vector of reflected ray, $\vec{T}$ is the directional vector of incident ray, $\vec{N}$ is the normal vector of the plane, t is the distance from starting point to plane, $\vec{P}$ is the position vector of plane, and $\vec{Q}$ is the position vector of the ray. Distance values which are less than zeros are eliminated first because it means the plane is on the opposite direction of the ray's traveling direction.

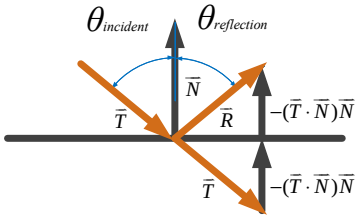

Figure 4: The law of reflection on ideal specular surface

The plane with minimum traveling distance is found and defined as the plane that the rays strike on. If the intercepted plane is one of the slats, then the ray flux will split to a specular portion and a diffuse portion using the shining factor. For the specular portion, the ray is being tracked continuously. The intersecting point becomes the new position vector of the ray which can be calculated by:

$$\vec{X} = \vec{Q} + t\vec{T} \tag{3}$$

where $\overline{X}$ is the position vector of the intersecting point and also the position vector of reflecting ray -the new directional vector is calculated by Eq. (3). The inter-reflections between the slats can reach high numbers; however, the direct luminous flux will diminish after each reflection due to the absorptance and the shining factor of slats. The equations in Fig. 5 show the remaining amount of luminous flux after striking the slat (σ is shining factor and ρ_{slat} is the slats direct reflectance). The maximum number of inter-reflections in this study was set to 10 and the left specular portion (which is small) is directly added to the direct-diffuse component in the 2-D radiosity calculation. The specular luminous flux that arrives on each interior surface is then studied in detail by dividing each surface into sub-surfaces (as explained in the 3-D room radiosity method section) and checking if the final strike positions are located within the boundaries of each sub-surface.

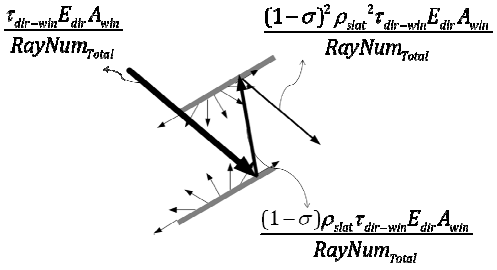

Figure 5: Inter-reflection process inside the slats using shining factors

2.2 Two-dimensional Radiosity Method for the Glass-Blind Cavity

The radiosity method proposed in EnergyPlus (2007) is used to obtain the diffuse transmitted and reflected amounts of light. For the transmitted diffuse component, the entering surface (S_1) is assumed to be a perfect diffuser as shown in Figure 6(a). This embeds an assumption that the transmittance of ground diffuse and sky diffuse components are equal. The other three surfaces are the upper slat (S_4), the bottom slat (S_3), and the "departing flux" surface (S_2). The slat is assumed to be infinite long. For the direct-diffuse component, two more surfaces are added. The slat surfaces are separated in two parts (Fig. 6b): S_3 is the slat length between the slat edge and the farthest point where direct rays strike. S_4 is the length between the slat edge and the nearest point that the rays reach on the second strike (the length of S_4 is zero in Fig. 6b). S_5 and S_6 are the remaining portions of the bottom and upper slats respectively. The amount of direct-diffuse component generated in each strike is decreased with more inter-reflections, so the remaining amount is small and it is added to the second strike and spread out to entire S_6 (the length that second strike achieves is shorter than S_6). As shown in Fig. 6(b), there is actually a third strike on S_5, which can be ignored and the flux amount of S_5 is added to S_6. The equations in Fig. 6 (b) show that the initial luminous exitance from S_3 is calculated from the diffuse luminous flux reflected on the first strike. The initial luminous exitance from S_6 is the sum of the diffuse luminous flux generated in the remaining strikes. The parameter $Ray_{bounce\text{-}j}$ determines if the strike happens at the j[th] bounce: if yes, it is set to 1; otherwise it is equal to zero.

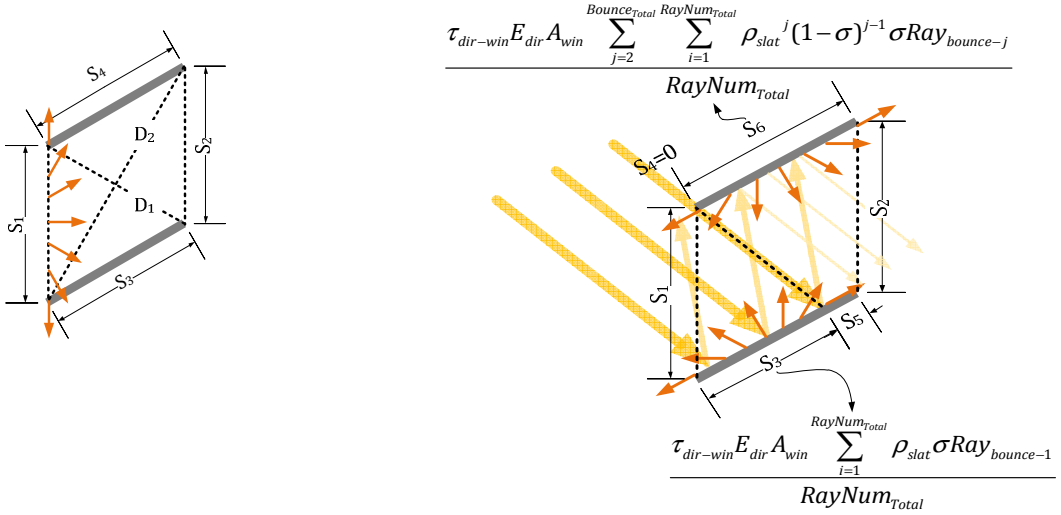

Figure 6: (a) The schema of original diffuse component; **(b)** The schema of direct-diffuse component

The view factors are then obtained as the equations below. For the rectangular cases such as S_1 and S_2 in Figure 6(a),

$$F_{12} = \frac{D_1 + D_2 - (S_1 + S_2)}{2S_1} \tag{4}$$

and for triangular case such as S_1 and S_3 in Figure 6(b)

$$F_{13} = \frac{S_1 + S_3 - D_1}{2S_1} \tag{5}$$

Then the radiosity J_i of segment S_i can be solved by

$$\mathbf{J} = X^{-1}\mathbf{Q} \tag{6}$$

$$X = \begin{bmatrix} 1 & 0 & 0 & 0 \\ 0 & 1 & 0 & 0 \\ -\rho_{slat}F_{13} & -\rho_{slat}F_{23} & 1 & -\rho_{slat}F_{43} \\ -\rho_{slat}F_{14} & -\rho_{slat}F_{24} & -\rho_{slat}F_{34} & 1 \end{bmatrix} \text{ or } \begin{bmatrix} 1 & 0 & 0 & 0 & 0 & 0 \\ 0 & 1 & 0 & 0 & 0 & 0 \\ -\rho_{slat}F_{13} & -\rho_{slat}F_{23} & 1 & -\rho_{slat}F_{43} & -\rho_{slat}F_{53} & -\rho_{slat}F_{63} \\ -\rho_{slat}F_{14} & -\rho_{slat}F_{24} & -\rho_{slat}F_{34} & 1 & -\rho_{slat}F_{54} & -\rho_{slat}F_{64} \\ -\rho_{slat}F_{15} & -\rho_{slat}F_{25} & -\rho_{slat}F_{35} & -\rho_{slat}F_{45} & 1 & -\rho_{slat}F_{65} \\ -\rho_{slat}F_{16} & -\rho_{slat}F_{26} & -\rho_{slat}F_{36} & -\rho_{slat}F_{46} & -\rho_{slat}F_{56} & 1 \end{bmatrix} \tag{7}$$

where **J** is the radiosity vector and **Q** is the vector of initial luminous flux. Finally, we can calculate the transmittance and reflectance of the original diffuse component as well as the direct-diffuse component (transmitted through blinds and reflected back to glass) from Eqs. (10-11):

$$\tau_{dif-blinds} = \sum_{j=1}^{4} J_j F_{j2} \quad \text{or} \quad DirectDiffuse_{trans} = \sum_{j=1}^{6} J_j F_{j2} \tag{8}$$

$$\rho_{dif-blinds} = \sum_{j=1}^{4} J_j F_{j1} \quad \text{or} \quad DirectDiffuse_{ref} = \sum_{j=1}^{6} J_j F_{j1} \tag{9}$$

where $\tau_{dif\text{-}blinds}$ is the diffuse transmittance and $\rho_{dif\text{-}slat}$ is the diffuse reflectance of the blind system. Then the portions reflected back to window are taken into consideration within the diffuse inter-reflection calculations between the glass and the blinds as explained above.

2.3 Three-dimensional Radiosity Method for Calculating Illuminance distributions in the Space

After solving the rays' proceedings inside the blinds, the 3-D radiosity method is employed to compute the final illuminance distributions on the work plane and on other interior surfaces. Each of the interior surfaces is first divided into small rectangular sub-surfaces with equal areas as shown in Fig. 7. A coarse mesh selection can speed up the calculation performance, and the fine mesh selection can give accurate and detailed results -that is a trade-off in calculation process. In this paper, we setup a mesh with 0.2m grid size. The uniformity of sub-surfaces can save time for calculating view factors. Only one set of view factors needs to be calculated even when we target annual problems. In each time step, the initial luminous exitance of each sub-surface of interior walls is calculated from the number of rays that strike on it as Eq. (12). For the sub-surfaces of blinds, all the diffuse parts (including the part with inter-reflections) will be added up to become the initial luminous exitance as shown in Eq. (13).

$$M_{0-n} = \frac{\tau_{dir-win}E_{dir}\sum_{i=1}^{RayNum_{total}}\left\{\left[\rho_{slat}(1-\sigma)\right]^{bounce}Ray_{n-i}\right\}}{RayNum_{total}} \times \frac{A_{window}}{A_{surface-n}} \times \rho_n \tag{10}$$

$$\begin{aligned} M_{0-m} = {} & E_{dif}\tau_{dif-win}\tau_{dif-blind} + DirectDiffuse_{trans} + \\ & \left\{ E_{dif}\tau_{dif-win}\rho_{dif-blind} + DirectDiffuse_{ref} + E_{dir}\tau_{dir-win}\frac{\sum_{i=1}^{RayNum_{total}}\left[\rho_{slat}(1-\sigma)Ray_{m-i}\right]}{RayNum_{total}} \right\} \\ & \times \frac{\rho_{dif-win}\tau_{dif-blind}}{1-\rho_{dif-blind}\rho_{dif-win}} \end{aligned} \tag{11}$$

where $M_{0\text{-}n}$ is the initial luminous exitance of sub-surface *n*, $M_{0\text{-}m}$ is the initial luminous exitance of blind sub-surface *m*, $A_{surface\text{-}i}$ is the area of sub-surface n, ρ_n is the reflectance of sub-surface n, E_{dif} is the incident diffuse illuminance, $Ray_{m\text{-}i}$ and $Ray_{n\text{-}i}$ determine if the i^{th} ray strikes on interior sub-surface *n* or on a window sub-surface *m*. After deciding the initial luminous exitance and finish with the ray-tracing calculations, the width of blinds is ignored. The

blinds can then treated as diffuse surfaces and put back to the position of glass as an integrated window system. The final luminous exitance of each sub-surface can finally be expressed as:

$$M_m = M_{0-m} + \sum_k^t (1 - abs_m) F_{km} M_k \quad (12)$$

where M_m is the final luminous exitance of surface m, , abs_m is the absorptivity of surface k, t is the total number of other surfaces, and F_{mk} is a view factor which is the fraction of flux emitted by surface k that falls on surface m. Instead of solving a large inverse matrix directly, a gathering algorithm was employed to solve the final illuminance distribution on work plane and interior surfaces by iteration.

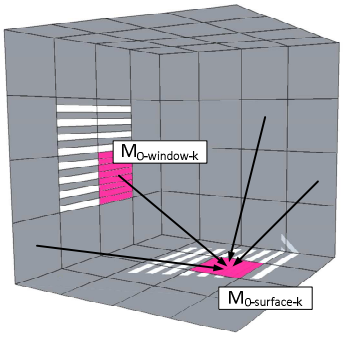

Figure 7: 3D-radiosity method schematic with sub-surfaces and direct components.

3. SIMULATION RESULTS

3.1 Comparison of Specular and Direct-Diffuse Blind Transmittance Results

Tables 1-2 present the blind transmittance (direct components) calculated with the hybrid method for two slat angles respectively, using as basic parameters 70% direct slat reflectance and 20% shining factor and compares the results with full radiosity calculations for different profile angles. The hybrid method consists of two parts, specular and diffuse, with amounts related to the shining factor and number of inter-reflections. When the slat angle is 0°, the diffuse part increases with profile angle since more bounces between blinds will occur. The specular-reflected part is always 0. When the slat angle is 45°, the specular part will be all reflected back to the window when the profile angle exceeds 45°. Figure 8 presents the total transmittance results (sum of specular and diffusely transmitted portions). The full radiosity method underestimates the transmittance in most of the cases because it ignores the directional effects of specular reflection. The maximum transmittance difference can be up to 35% which can translate into significant accuracy problems in lighting simulation.

Table 1: Transmittance of direct components when slat angle is 0°

	Hybrid					**Radiosity**			
	Specular		Diffuse		Total	Direct			Total
Profile Angle	Transmitted (fig.2a&c)	Reflected to glass (fig.2b)	Transmitted (eq.10)	Reflected to glass (eq.11)	Transmitted	Direct-Direct	Direct-Diffuse	Reflected to glass	Transmitted
10	0.92	0.00	0.00	0.00	0.92	0.82	0.05	0.05	0.87
20	0.84	0.00	0.01	0.01	0.85	0.64	0.11	0.11	0.74
30	0.75	0.00	0.03	0.03	0.78	0.42	0.17	0.17	0.59
40	0.63	0.00	0.07	0.07	0.70	0.16	0.24	0.24	0.40
50	0.51	0.00	0.12	0.13	0.63	0.00	0.27	0.31	0.27
60	0.38	0.00	0.16	0.17	0.54	0.00	0.23	0.34	0.23
70	0.21	0.00	0.20	0.18	0.42	0.00	0.20	0.36	0.20
80	0.04	0.00	0.23	0.16	0.27	0.00	0.17	0.38	0.17

3.2 Work plane Illuminance Calculation and Comparison of Results

The developed hybrid method was used to calculate illuminance distributions in a 4m x 4m x 3m high perimeter office located in Philadelphia, PA and demonstrate the potential of utilizing this method for building simulation and estimation of daylighting availability, potential energy savings from lighting controls, as well as impact on energy performance of perimeter zones with venetian blinds and prediction of potential glare problems. The façade is facing south and the window dimensions are 1m high x 1.6m wide, centered on the exterior façade. A double-glazed clear window was used (normal visible transmittance=0.786, diffuse transmittance=0.68). The angular transmission and reflection properties of the glass were considered according to data provided by WINDOW 6. The window is

equipped with interior venetian blinds of 70% reflectance and shining factor equal to 20%. The width of the slats was 0.1m, equal to the spacing between them. Results are presented for two representative days (Jan 21st and June 21st) and two representative times (9am and 12pm) with sky conditions generated based on the CIE clear sky model.

Table 2: Transmittance of direct components when slat angle is 45°

	Hybrid					**Radiosity**			
	Specular		Diffuse		Total	Direct			Total
Profile Angle	Transmitted (fig.2a&c)	Reflected to glass (fig.2b)	Transmitted (eq10)	Reflected to glass (eq11)	Transmitted	Direct-Direct	Direct-Diffuse	Reflected to glass	Transmitted
10	0.37	0.11	0.12	0.13	0.48	0.13	0.17	0.39	0.30
20	0.22	0.20	0.14	0.17	0.36	0.15	0.04	0.45	0.18
30	0.11	0.32	0.11	0.18	0.22	0.14	0.00	0.49	0.14
40	0.01	0.47	0.09	0.16	0.10	0.12	0.00	0.51	0.12
50	0.00	0.56	0.07	0.14	0.07	0.11	0.00	0.53	0.11
60	0.00	0.56	0.07	0.12	0.07	0.09	0.00	0.55	0.09
70	0.00	0.56	0.06	0.11	0.06	0.08	0.00	0.57	0.08
80	0.00	0.56	0.05	0.09	0.05	0.07	0.00	0.59	0.07

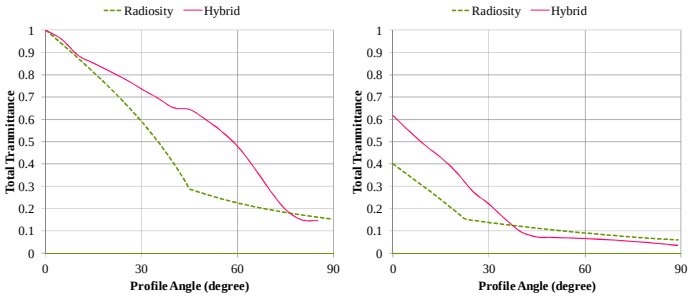

Figure 8: (a) Total transmittance as a function of the profile angle (originating from direct components only) and comparison between the hybrid and the radiosity methods when the slat angle is 0° **(b)** when the slat angle is 45°.

The left part of Fig. 9 presents the illuminance distribution on interior surfaces and on the work plane using the hybrid method, and the right part 9 presents the final striking positions of directly-reflected rays. Figure 9(a) shows the results at Jan 21th 9:00am and the slat angle is 0° (horizontal). In this case the rays strike on the west wall not on the floor; however the work plane area receives direct light. This scenario results in high illuminance on every interior surface and will create glare problems. Comparing the results of Figure 9(a) and Figure 9(b), the transmittance when slat angle is 0° is higher than the transmittance when the slat angle is 45°. In Figure 9(b), part of the rays is reflected back to outside when slats are tilted at 45°. A particularly important case is presented next: Figure 9(c) is the same setup at 12:00 pm; outside illuminance is very high and the profile angle is small in this case. Although the slat position is located in 45°, part of the rays are transmitted back to outside, and two bounces happened between the slats. The intensity of rays does not scatter enough before entering the room due to the high specular properties and low shining factors. The final arrived position of rays is the floor, (not the ceiling) since the rays strike on bottom slats first and then reflected to the upper slats without any more inter-reflections. This changes the directional vector towards the work plane which will cause serious glare problems. Figure 4(d) is the same case in summer and the slat angle is 45°. All the direct light is reflected back to outside due to the high profile angle.

4. CONCLUSIONS

This paper presented a newly developed hybrid ray-tracing and radiosity method for spaces equipped with venetian blinds. It extracts the advantages of both ray tracing and radiosity methods - the accuracy of ray tracing when simulating specular characteristics and also the rapid simulation speed of radiosity when simulating diffuse characteristics. It can lead to a useful decision-making tool in both early design stage and operation stage. For the early design stage, the enhanced speed supports the designer to test different cases with daily and annual results. For operating stage, the building manager or occupancy can implement both daylighting and shading controls through the detailed prediction of surface illuminance. Further studies related to annual simulation, control algorithms and validation with experimental results need to be conducted and expand the potential of the model.

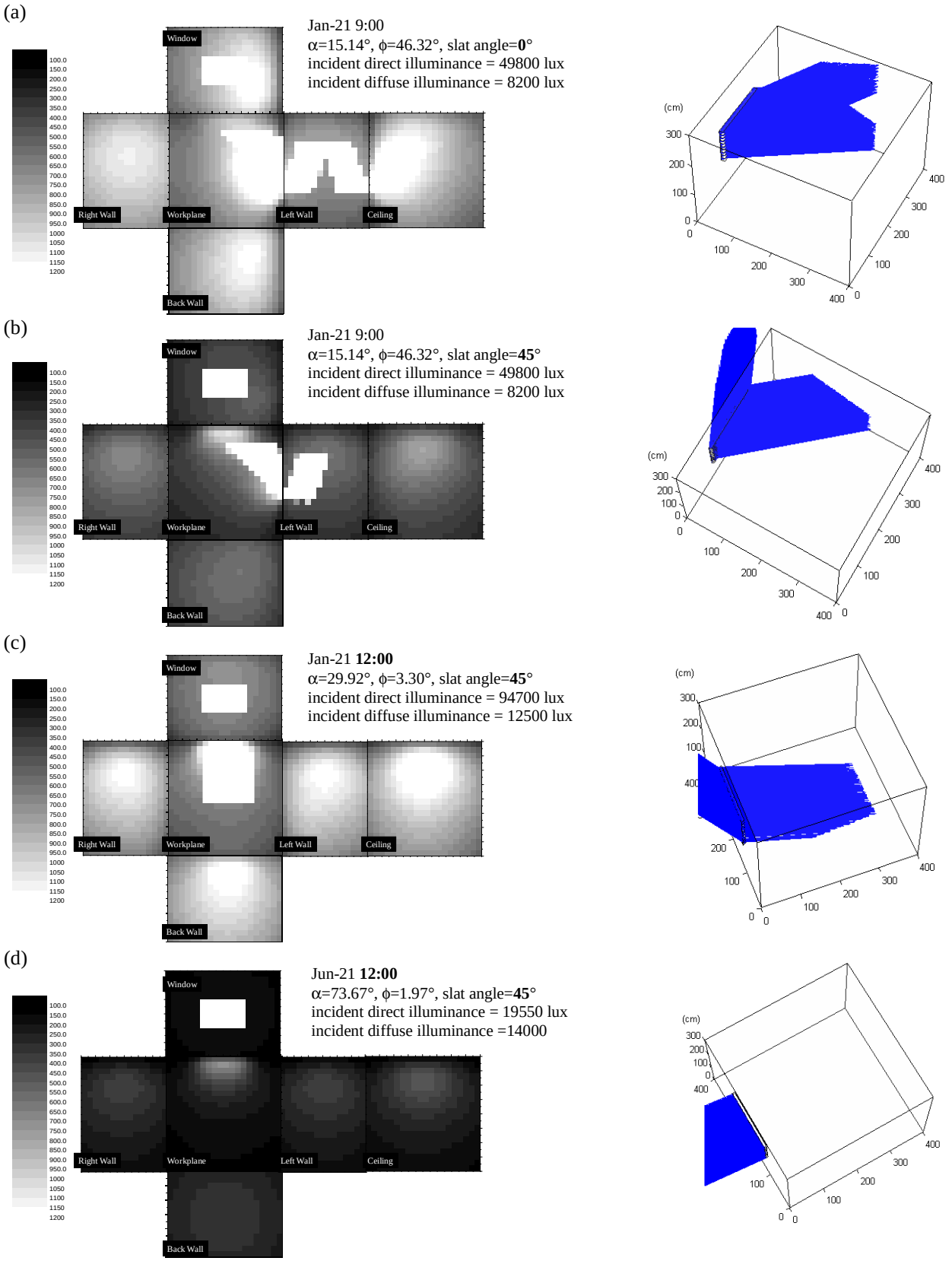

Figure 9: (a) Illuminance distribution contours on Jan-21 9:00 with 0° slat angle; **(b)** Jan-21 9:00 with 45° slat angle; **(c)** Jan-21 12:00 with 45° slat angle; **(d)** Jun-21 12:00 with 45° slat angle;

REFERENCES

Andersen, M. de Boer, J., 2006, Goniophotometry and Assessment of Bidirectional Photometric Properties of Complex Fenestration Systems. *Energ. Buildings*, vol. 38, no. 7: p. 836-848.

Andersen, M., Rubin, M., Powles, R. Scartezzini, J.L., 2005, Bi-Directional Transmission Properties of Venetian Blinds: Experimental Assessment Compared to Ray-Tracing Calculations. *Sol. Energy*, vol. 78, no. 2: p. 187-198.

Breitenbach, J., Lart, S., Längle, I. Rosenfeld, J.L.J., 2001, Optical and Thermal Performance of Glazing with Integral Venetian Blinds. *Energ. Buildings*, vol. 33, no. 5: p. 433-442.

Campbell, N.S. Whittle, J.K., 1997. Analyzing Radiation Transport through Complex Fenestration Systems. In *5th IBPSA conference*, 173-180. Prague Czech Repblic.

Chaiyapinunt, S. Worasinchai, S., 2009, Development of a Mathematical Model for a Curved Slat Venetian Blind with Thickness. *Sol. Energy*, vol. 83, no. 7: p. 1093-1113.

ISO. 2003. Iso 15099:2003(E). In *Thermal performance of windows, doors and shading devices - Detailed calculations*. Geneva, Switzerland: International Organization for Standardization.

Klems, J.H. Warner, J.L., 1995, Measurement of Bi-Directional Optical Properties of Complex Shading Devices. *ASHRAE Tran.*, vol. 101, no. 1: p. 791-801.

Kotey, N.A., Collins, M.R., Wright, J.L. Jiang, T., 2009, A Simplified Method for Calculating the Effective Solar Optical Properties of a Venetian Blind Layer for Building Energy Simulation. *J. Sol. Energ.*, vol. 131, no. 2: p. 021002.

LBNL. 2007. *Energyplus Engineering Reference—the Reference for Energyplus Calculations*. Lawrence Berkeley National Laboratory (LBNL).

Lehar, M.A. Glicksman, L.R., 2007, Rapid Algorithm for Modeling Daylight Distributions in Office Buildings. *Build. Environ.*, vol. 42, no. 8: p. 2908-2919.

Parmelee, G.V. Aubele, W.W., 1952, The Shading of Sunlit Glass: An Analysis of the Effect of Uniformly Spaced Flat Opaque Slats. *ASHVE Transactions*, vol. 58: p. 377-398.

Pfrommer, P., Lomas, K.J. Kupke, C., 1996, Solar Radiation Transport through Slat-Type Blinds: A New Model and Its Application for Thermal Simulation of Buildings. *Sol. Energy*, vol. 57, no. 2: p. 77-91.

Robinson, D. Stone, A., 2006, Internal Illumination Prediction Based on a Simplified Radiosity Algorithm. *Sol. Energy*, vol. 80, no. 3: p. 260-267.

Rosenfeld, J.L.J., Platzer, W.J., van Dijk, H. Maccari, A., 2001, Modelling the Optical and Thermal Properties of Complex Glazing: Overview of Recent Developments. *Sol. Energy*, vol. 69, Supplement 6, no. 0: p. 1-13.

Simmler, H. Binder, B., 2008, Experimental and Numerical Determination of the Total Solar Energy Transmittance of Glazing with Venetian Blind Shading. *Build. Environ.*, vol. 43, no. 2: p. 197-204.

Tsangrassoulis, A., Niachou, K., Papakostantinou, N., Pavlou, C. Santamouris, M., 2002, A Numerical Method to Estimate Time-Varying Values of Diffuse Irradiance on Surfaces in Complex Geometrical Environments. *Renew. Energ.*, vol. 27, no. 3: p. 427-439.

Tzempelikos, A., 2008, The Impact of Venetian Blind Geometry and Tilt Angle on View, Direct Light Transmission and Interior Illuminance. *Sol. Energy*, vol. 82, no. 12: p. 1172-1191.

Versluis, R., 2005. Ray-Tracing Vs. Radiosity Modeling of Venetian and Pleated Blinds and the Influence of the Energetic Properties of Windows. In *IBPSA-NVL Conference*. Delft, Netherlands

Ward, G. Shakespeare, R., 1998. *Rendering with Radiance. The Art and Science of Lighting Visualization*. Morgan Kaufmann Publishers.

Ward, G.J., 1992, Measuring and Modeling Anisotropic Reflection. *Comp. Graph.*, vol. 26, no. 2.

ACKNOWLEDGMENT

This work is funded by Energy Efficient Buildings Hub, sponsored by the US Department of Energy under Award Number DE-EE0004261.